A&A 399, L5–L9 (2003)
DOI: 10.1051/0004-6361:20030016

Astronomy & Astrophysics

Letter to the Editor

On the outflow in an equatorial coronal hole

L. D. Xia, E. Marsch, and W. Curdt

Max-Planck-Institut für Aeronomie, 37191 Katlenburg-Lindau, Germany

Received 29 November 2002 / Accepted 7 January 2003

Abstract. We report new observations concerning the source of the fast solar wind by directly comparing Doppler-shift maps of Ne^{7+} with charts of the photospheric magnetic field in an equatorial coronal hole, which was observed by SUMER/SOHO and NSO/Kitt Peak on November 5, 1999. The relationship between the velocity field, line intensity and magnetic network is discussed. Our data show that there are both dark and bright regions in this coronal hole as seen in the Ne VIII line. The larger blue shifts of the Ne VIII line are associated mainly with the darker region, where the strong magnetic flux with a single polarity is concentrated. Conversely, the smaller blue shifts are measured mainly in the brighter region, with an underlying mixed-polarity magnetic structure. These observational results are in agreement with the model prediction that the fast solar wind is initially accelerated in the coronal funnels, which are regions with globally open coronal fields rooted in the magnetic network.

Key words. Sun: corona – Sun: solar wind – Sun: UV radiation – Sun: magnetic fields

1. Introduction

It has long been known that the coronal holes are the source of the fast solar wind (see, e.g., Krieger et al. 1973). In the large-scale open fields, which are rooted on the Sun's surface in the magnetic network and expand from there outward into the interplanetary space, the coronal plasma can be quickly accelerated and become supersonic within several solar radii. However, it still remains unknown how the fast solar wind starts initially in the transition region and at the coronal base. Some authors have suggested (Marsch & Tu 1997; Hackenberg et al. 2000; Vocks & Marsch 2002) that the nascent fast solar wind may first be accelerated in magnetic funnels, which are named after the notion that the open magnetic fields are at low altitude concentrated at the boundaries of the supergranulation cells, created by the convective motion of the photospheric material, but then expand quickly with height from the transition region into the lower corona and attain a funnel shape (Gabriel 1976; Dowdy et al. 1986) due to the changing equilibrium between the magnetic and thermal pressure in the gravitationally stratified solar atmosphere (see, e.g., Hackenberg et al. 2000).

With the high spectral resolution of the SUMER (Solar Ultraviolet Measurements of Emitted Radiation) instrument onboard the Solar and Heliospheric Observatory (SOHO), Doppler shifts of spectral lines can be measured with an accuracy of about 2 km s^{-1} (SUMER has spectral resolution elements of 42–45 mÅ and can, by centroiding, achieve subpixel resolution). Such work has been done by many authors in quiet-Sun regions and polar coronal holes (PCHs) of the Sun (see, e.g., Brekke et al. 1997; Hassler et al. 1999; Peter 1999; Wilhelm et al. 2000). In PCHs, the average Doppler shift of the Ne VIII (770 Å) line and the relationship between Doppler shift and chromospheric network has been studied by Hassler et al. (1999). They found strong evidence that the largest outflow velocities are closely associated with the underlying chromospheric network, whereby they used the Si II (1533 Å) brightenings in the radiance image as an indication of the chromospheric magnetic network. An extended work, done by Stucki et al. (2000), who did a statistical analysis, showed a positive correlation between the blue shift of the Ne VIII line and the intensity of the N IV line (765 Å) (used also as an indicator of the network) in the polar coronal hole, and thus corroborated the results of Hassler et al. (1999). Another interesting observational result is that the largest blue shifts of the Ne VIII line coincide spatially with very dark regions in the intensity image of the coronal hole when seen in the same line (Wilhelm et al. 2000).

In this letter, we present new observations concerning the source of the fast solar wind, by a direct comparison of the deduced velocity field with the measured photospheric magnetic field in an equatorial coronal hole (CH). The motivation for this work is twofold. First, the previous studies were carried out in PCHs. In this case the line-of-sight geometry is restricted, which may lead to an underestimation of the plasma velocity and greater uncertainty of the magnetic field measurements than at the solar equator. Second, only data from spectral measurements were used in the previous studies. We show here that an analysis combining SUMER spectroscopic data with magnetic field maps can give us a clearer physical picture of the plasma conditions and flow pattern prevailing at the coronal hole base.

Send offprint requests to: L. D. Xia, e-mail: xia@linmpi.mpg.de

2. Observations and data analysis

During the period November 3–8, 1999, the SUMER telescope was pointed to a large equatorial coronal hole and traced the darkest parts with raster scans. The selected spectral window was centered around 1540 Å, which includes lines of Si II (1533 Å), C IV (1548 Å and 1550 Å) and Ne VIII (770 Å in 2nd order). The formation temperatures of these lines span from about 1.8×10^4 K to 6.3×10^5 K. The lines are emitted in the upper chromosphere, transition region and coronal base, respectively.

The SUMER data selected for this study were taken on November 5. The instrument has been described in detail elsewhere (Wilhelm et al. 1995; Wilhelm et al. 1997). The detector A and slit 2 with a size of $1'' \times 300''$ were used. SUMER began to raster in East-West direction at 470″ E and ended at 185″ E (solar disk coordinates). The corresponding times are 17:07 UT and 21:07 UT, respectively. A 150 s exposure time and 3″ raster step size were selected. The slit's center was pointed at 160″ N during the whole scan. The total data set consists of 96 exposures. This coronal hole is shown in Fig. 1 (left panel, see caption for further explanations).

Previous studies (Huber et al. 1974; Bohlin 1977) have shown that the chromospheric network in coronal holes is nearly absent when observed in lines with formation temperatures above 5×10^5 K (e.g., in the Ne VIII and Mg IX lines with SUMER, Hassler et al. 1999; Wilhelm et al. 2000; Wilhelm et al. 2002). Therefore, we can use the lines Ne VIII (770 Å) observed by SUMER and Fe XII (195 Å) observed by the Extreme ultraviolet Imaging Telescope (EIT) on SOHO to determine the coronal hole boundary. The hole under study here appeared as a dark region in all three EIT coronal images. Its boundary is outlined in Fig. 1 by a white dotted line. The overlaid box-shaped window indicates the field of view (FOV) of SUMER, which covered an area of about 252×300 arcsec^2 (1 arcsec equals about 715 km on the Sun's surface seen from SOHO's orbit). It should be mentioned that SUMER rastered along the East-West direction, which is in the sense of the Sun's rotation, and therefore the effective field of view in this direction becomes smaller.

In our analysis of the SUMER spectra, we first applied the standard procedures for correcting and calibrating the data. Two methods were then applied to get the central position of lines. First, we fitted the average profile to a single Gaussian or multi-Gaussians, thereby using the PIKAIA software (Charbonneau 1995). Second, in order to deduce the Dopplergrams we calculated the central position for every pixel, by integrating the line intensity across a certain spectral window and determining subsequently the location of the 50% level with sub-pixel accuracy. This procedure was frequently used to obtain SUMER Dopplergrams (see in details, Dammasch et al. 1999) and dramatically reduced the computing time for a large number of data. However, a systematic deviation of deduced central positions would exist if the selected spectral window included other lines. This deviation can be corrected by comparing the average position deduced by this method with that obtained by the multi-Gaussian fitting. We found that the results deduced by two methods are statistically consistent with each other.

Furthermore, it should be mentioned that in addition a line-position correction was performed, to remove spurious spectral line shifts caused by thermal deformations of the instrument, and to eliminate residual errors (systematically varying along the slit) after the geometric correction using the standard software.

We have used cold chromospheric lines as reference lines in order to achieve an absolute wavelength calibration. Spectral lines with known, accurate laboratory wavelengths, such as lines of Si I, Si II and C I, are most appropriate for this purpose. They have relatively low formation temperatures. This calibration method is very useful for observations on the disk. Previous studies have shown that chromospheric lines have only very small systematic line shifts on average. For example, Hassler et al. (1991) found the absolute shift of Si II (1533 Å) to be only 0 ± 1.2 km s^{-1}, comparing the solar lines with those of an on-board calibration lamp. For the C I line (Chae et al. 1998) only a small average red shift of about 1.5 km s^{-1} has been estimated. Consequently, such lines can be used as references to establish a wavelength coordinate along the dispersion direction. Shifts of other lines can then be calculated by comparison with the calibration lines. The estimated accuracy is about 2 km s^{-1}, as many authors have confirmed (see, e.g., Brekke et al. 1997; Chae et al. 1998; Peter 1999; Dammasch et al. 1999). In addition, we adopted a wavelength of 770.428 Å as the rest wavelength of the Ne VIII line, which seems to be the most accurate value obtained by using SUMER data (Dammasch et al. 1999; Peter 1999).

In this study, the photospheric magnetogram was obtained by anonymous ftp from the NSO (National Solar Observatory) at Kitt Peak. The used Fe I (8688 Å) magnetogram was taken between 17:48 UT and 18:43 UT on the same day, with spatial resolution elements of 1.14×1.14 arcsec^2. Following the documentation on the magnetic field data, we have multiplied the instrumental values by a factor of 1.46, thus converting them to magnetic field strength given in Gauss. A detailed description of the measurement has been given in Jones et al. (1992). We finally co-aligned the magnetogram and the SUMER image in the Si II line by computing the cross correlation between the two images.

3. Results

Before discussing the relationship between the chromospheric network and the plasma flow deduced from Doppler shifts, we check the correspondence between the measured magnetogram and EUV images. In Fig. 1 (middle and right panels), we plot together the spectral radiance maps obtained by SUMER in the Si II and Ne VIII lines and magnetic field maps (contours with levels of −30 G, −15 G, 15 G and 30 G) measured by NSO/Kitt Peak. In Fig. 1 (middle panel), the network structure (seen as a bright pattern in the Si II line) corresponds to the concentrations of magnetic flux. The magnetic network structure in this coronal hole is very stable during the SUMER observation, and the image of the Si II brightness and the magnetic network are well coinciding spatially. The magnetic map

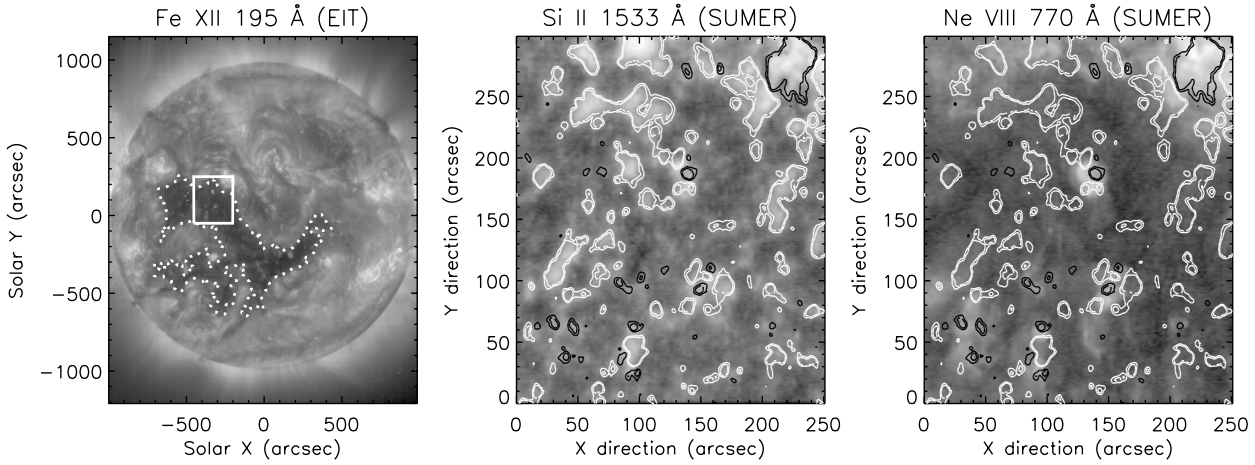

Fig. 1. Left panel: An equatorial coronal hole as seen in the 195 Å channel of EIT, with the field-of-view of SUMER being superimposed as a white box. Middle and right panels: Image scanned by SUMER covering a part of this hole as seen in the Si II (1533 Å) and Ne VIII (770 Å in 2nd order) lines, respectively. Contour plots in the middle and right panels represent magnetograms of the same area observed by NSO/Kitt Peak, with the white lines representing the positive polarity of the line-of-sight field component and the black line the negative polarity. The chromospheric network is indicated by the intensity of the cooler line of Si II and by the magnetic field. Both data sets are consistent with each other.

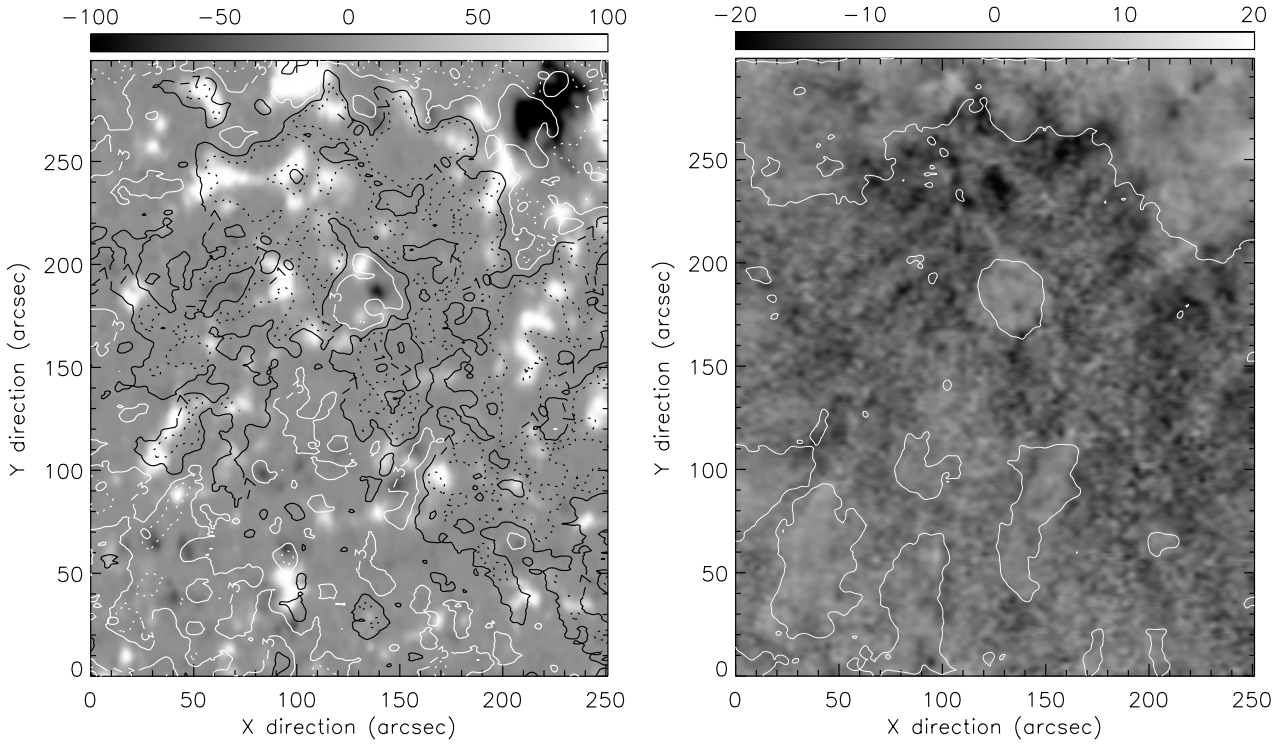

Fig. 2. Left panel: Magnetogram (white: positive polarity; black: negative polarity; full scale: ±100 G) with overlaid contour plots of Doppler shifts in km s^{-1}, with the cool line C I (1542 Å) as the reference line for the Ne VIII line (black dotted: −10, black solid: −7, white solid: −3, and white dotted: 0 km s^{-1}). Right panel: Doppler shifts (full scale: ±20 km s^{-1}) of the Ne VIII line with overlaid contour plots of its intensity. Note that the upper part of the image is outside of the coronal hole. For Doppler shifts, negative values denote blue shifts, while positive red shifts.

indicates that this hole is occupied predominantly by white patches indicating positive polarity of the field. The average net magnetic flux density (signed) is about 7 G inside the hole, with an uncertainty of less than 1 G (J. Harvey, private communication). There were also some mixed-polarity magnetic features in this CH (see also the left panel of Fig. 2). The negative flux occupied about 25% of the total unsigned flux in the CH area.

Note that by means of the Si II brightness alone, we are not able to distinguish the polarity of the field. Both polarities are present, but they cannot be discriminated, since both types of fields appear as similar, bright plasma features when seen in this chromospheric line. However, the image of the Ne VIII radiance (Fig. 1, right panel) shows that in this line the network structure is almost invisible inside the CH, except for some

isolated bright points (BPs). Such bright points can be identified well in images of the Ne VIII line, and also in coronal lines observed by EIT, and are associated spatially with regions where mixed-polarity magnetic features are present. The relative area occupied by such bright points is estimated to be about 14%. The intensity ratio between bright points and dark regions is on average about 3.3 for the Ne VIII line.

In Fig. 2, we plot the magnetogram together with contours of the Doppler shift of the Ne VIII line (left panel), and the Doppler-shift map together with contours of the intensity of the Ne VIII line (right panel). The velocity field is quite inhomogeneous over the whole field of view (see right panel). Therefore, we smoothed the deduced velocity map over six adjacent pixels, before the contours of the Doppler shift were actually plotted, in order to show its distribution more clearly. The observed features of this CH can be divided into three groups: small active regions outside the hole (upper part of the image), and bright and dark regions inside the hole. In order to separate these three regions, we first deduced the intensity histogram of the Ne VIII line across the whole image (spectroheliogram). This distribution can be considered to be roughly composed by two components: one contributed by dark regions and another with high intensities by bright regions inside and outside the hole. A threshold of the intensity was then determined, by help of which the boundaries of the three regions are marked by plotting contours (see right panel). The line is predominantly blue shifted in the observed area, and its average blue shift in relation to the C I line (1542.1766 Å) is found to be 3 $\mathrm{km\,s^{-1}}$ outside the hole, 4 $\mathrm{km\,s^{-1}}$ in the bright region and 7.5 $\mathrm{km\ s^{-1}}$ in the dark region.

The contours of the Doppler shift show a close relationship with the magnetic network structure inside the hole. Larger blue shifts with speeds above 10 $\mathrm{km\,s^{-1}}$ (black dotted line) are mainly associated with regions where the magnetic field is concentrated in a single polarity (positive). As a simple statistical result, the net signed flux density of the underlying field is estimated to be about 11 G, 8 G and 4 G for blue shifts above 10 $\mathrm{km\,s^{-1}}$, between 10 and 7 $\mathrm{km\,s^{-1}}$ and between 7 and 3 $\mathrm{km\,s^{-1}}$, respectively. On the other hand, smaller blue shifts with speeds below 3 $\mathrm{km\,s^{-1}}$ (white solid line) occur mainly in the dispersed mixed-polarity network, which is also associated with the bright points seen in the Ne VIII line.

4. Summary and discussion

We have deduced an outflow velocity map of the Ne^{7+} ion from shifts of the Ne VIII 770 Å resonance line in an equatorial coronal hole, which was observed by SUMER/SOHO on November 5, 1999. This Dopplergram has been compared with the photospheric magnetic field measured by NSO/Kitt Peak in the same CH area. Our data show that there are both dark and bright regions in this coronal hole as seen in the Ne VIII line. The larger blue shifts are mainly associated with the dark regions, where the strong magnetic flux of a single polarity is concentrated. Conversely, smaller blue shifts stem mainly from the bright regions, with mixed-polarity magnetic structures underlying. These observational results are in agreement with the notion that the fast solar wind is initially accelerated in open magnetic funnels. The measured outflow velocity in the central region of the network is comparable with the model prediction (see discussion below).

Some modelling work has been done to study the physical properties of a coronal funnel. Coronal heating and acceleration was considered as being due to cyclotron damping of Alfvén waves and thrusting by Alfvén wave pressure (e.g., Marsch & Tu 1997; Hackenberg et al. 2000; Li 2002; Vocks & Marsch 2002). The resulting plasma properties depend largely on the geometry of the funnel and the details of the wave energy transport and dissipation process. According to these studies, the plasma can be driven to a flow speed of several tens $\mathrm{km\,s^{-1}}$, essentially by a large thermal pressure gradient at the base of the funnel. This pressure gradient results from the quick expansion of the magnetic flux tube, causing rapid heating with height through the high-frequency wave sweeping (resonant absorption).

Finally, we will estimate the possible contribution of bright points to the total outward mass flux under the assumption that the deduced Doppler shift of the Ne VIII line represents the real outflow velocity of the Ne^{7+} ions which are markers of the proton flow. Then we have,

$$f_{\mathrm{tot}} = f_{\mathrm{bp}} + f_{\mathrm{dr}} = N_{\mathrm{e,bp}} v_{\mathrm{bp}} A_{\mathrm{bp}} + N_{\mathrm{e,dr}} v_{\mathrm{dr}} A_{\mathrm{dr}}, \quad (1)$$

where f, v and A are the mass flux, deduced outflow velocity and flux tube area. $N_{\mathrm{e,bp}}$ and $N_{\mathrm{e,dr}}$ denote the electron density in bright points and dark regions. Their ratio can be estimated by the line intensity ratio, if we simply assume the emission volume (having the same bottom area) is the same for a given line in bright points and dark regions of the hole. Thus, we find that

$$\frac{N_{\mathrm{e,bp}}}{N_{\mathrm{e,dr}}} \approx \sqrt{\frac{I_{\mathrm{bp}}}{I_{\mathrm{dr}}}} \approx 1.8. \quad (2)$$

The mass flux contributed by bright points to the total outflow within the measured hole area, $f_{\mathrm{bp}}/f_{\mathrm{tot}}$, is then estimated to be about 11%. It should be mentioned that we have subtracted a value of 1.5 $\mathrm{km\,s^{-1}}$ from the deduced velocity due to the average red shift of the C I line itself. This estimate of the mass flux by measuring the Doppler shift is consistent with the previous estimate obtained for polar plumes by Wang (1994), and suggests that the portion of the mass flux contributed by bright points to the fast solar wind is at most comparable to their areal ratio and thus negligible.

Further work is presently being done by analysing more data in search for a correlation between the magnetic flux density and outflow velocity, because we expect that the characteristics of the magnetic field, e.g. the flux tube geometry, will have direct effects on the plasma properties of the nascent fast solar wind.

Acknowledgements. The SUMER project is financially supported by DLR, CNES, NASA and the ESA PRODEX program (Swiss contribution). We thank the EIT team for use of their data. SUMER and EIT are part of SOHO, which is a mission of ESA and NASA. NSO/Kitt Peak data used here are produced cooperatively by NSF/NOAO, NASA/GSFC, and NOAA/SEL. We would like to thank Dr. K. Wilhelm and I. E. Dammasch for helpful discussions on SUMER data analysis.

References

Brekke, P., Hassler, D. M., & Wilhelm, K. 1997, Sol. Phys., 175, 349
Bohlin, J. D. 1977, Sol. Phys., 51, 377
Chae, J., Yun, H. S., & Poland, A. I. 1998, ApJS, 114, 151
Charbonneau, P. 1995, ApJS, 101, 309
Dammasch, I. E., Wilhelm, K., Curdt, W., et al. 1999, A&A, 346, 285
Dowdy, J. F., Rabin, D., & Moore, R. L. 1986, Sol. Phys., 105, 35
Gabriel, A. H. 1976, Phil. Trans. Roy. Soc. Lond. A., 281, 339
Hackenberg, P., Marsch, E., & Mann, G. 2000, A&A, 360, 1139
Hassler, D. M., Rottman, G. J., & Orrall, F. Q. 1991, ApJ, 372, 710
Hassler, D. M., Dammasch, I. E., Lemaire, P., et al. 1999, Science, 283, 810
Huber, M. C. E., Foukal, P. V., Noyes, R. W., et al. 1974, ApJ, 194, L115
Jones, H. P., Duvall, Jr. T. L., Harvey, J. W., et al. 1992, Sol. Phys., 139, 211
Krieger, A. S., Timothy, A. F., & Roelof, E. C. 1973, Sol. Phys., 29, 505
Li, X. 2002, ApJ, 571, L67
Marsch, E., & Tu, C.-Y. 1997, Sol. Phys., 176, 87
Peter, H. 1999, ApJ, 522, 1148
Stucki, K., Solanki, S. K., Schühle, U., et al. 2000, A&A, 362, L49
Vocks, C., & Marsch, E. 2002, ApJ, 568, 1030
Wang, Y.-M. 1994, ApJ, 435, L153
Wilhelm, K., Curdt, W., Marsch, E., et al. 1995, Sol. Phys., 162, 189
Wilhelm, K., Lemaire, P., Curdt, W., et al. 1997, Sol. Phys., 170, 75
Wilhelm, K., Dammasch, I. E., Marsch, E., et al. 2000, A&A, 353, 749
Wilhelm, K., Dammasch, I. E., & Xia, L. 2002, Adv. Space Res., 30, 517